Real-time, contrast enhanced photoacoustic imaging of cancer in a mouse window chamber

Ragnar Olafsson*, Daniel R. Bauer, Leonardo G. Montilla, and Russell S. Witte

Department. of Radiology, University of Arizona, Tucson, AZ 85724, USA
**rolafsso@email.arizona.edu*

Abstract: A clinical ultrasound scanner and 14 MHz linear array collected real-time photoacoustic images (PAI) during an injection of gold nanorods (GNRs) near the region of a mature PC-3 prostate tumor in mice implanted with a skin flap window chamber. Three dimensional spectroscopic PAI (690-900nm) was also performed to investigate absorption changes near the tumor and enhance specific detection of GNRs. Whereas GNRs improved PAI contrast (+ 18 dB), the photoacoustic spectrum was consistent with the elevated near infrared absorption of GNRs. The versatile imaging platform potentially accelerates development of photoacoustic contrast agents and drug delivery for cancer imaging and therapy.

OCIS codes: (170.3880) Medical and biological imaging; (170.6510) Spectroscopy, tissue diagnostics; (170.1870) Dermatology; (110.7170) Ultrasound; (170.5120) Photoacoustic imaging.

References and links

1. A. Jemal, R. Siegel, E. Ward, Y. P. Hao, J. Q. Xu, and M. J. Thun, "Cancer statistics, 2009," CA Cancer J. Clin. **59**(4), 225–249 (2009).
2. E. D. Agdeppa, and M. E. Spilker, "A review of imaging agent development," AAPS J. **11**(2), 286–299 (2009).
3. G. H. Algire, and F. Y. Legallais, "Recent developments in the transparent-chamber technique as adapted to the mouse," J. Natl. Cancer Inst. **10**(2), 225–253, 8 (1949).
4. G. H. Algire, and J. U. Schlegel, "Circulatory reactions in photodynamic action," J. Cell. Comp. Physiol. **35**(1), 95–110 (1950).
5. Q. Huang, S. Q. Shan, R. D. Braun, J. Lanzen, G. Anyrhambatla, G. H. Kong, M. Borelli, P. Corry, M. W. Dewhirst, and C. Y. Li, "Noninvasive visualization of tumors in rodent dorsal skin window chambers," Nat. Biotechnol. **17**(10), 1033–1035 (1999).
6. L. Y. Chen, L. S. Gobar, N. G. Knowles, D. W. Wilson, and H. H. Barrett, "Direct Charged-Particle Imaging System Using an Ultra-Thin Phosphor: Physical Characterization and Dynamic Applications," IEEE Trans. Nucl. Sci. **56**(5), 2628–2635 (2009).
7. M. W. Dewhirst, E. T. Ong, R. D. Braun, B. Smith, B. Klitzman, S. M. Evans, and D. Wilson, "Quantification of longitudinal tissue pO2 gradients in window chamber tumours: impact on tumour hypoxia," Br. J. Cancer **79**(11/12), 1717–1722 (1999).
8. A. Mariampillai, B. A. Standish, E. H. Moriyama, M. Khurana, N. R. Munce, M. K. K. Leung, J. Jiang, A. Cable, B. C. Wilson, I. A. Vitkin, and V. X. D. Yang, "Speckle variance detection of microvasculature using swept-source optical coherence tomography," Opt. Lett. **33**(13), 1530–1532 (2008).
9. R. A. Gatenby, E. T. Gawlinski, A. F. Gmitro, B. Kaylor, and R. J. Gillies, "Acid-mediated tumor invasion: a multidisciplinary study," Cancer Res. **66**(10), 5216–5223 (2006).
10. A. F. Gmitro, Y. Lin, and M. Farrokh, "A System for Multi-Modality Optical and MR Imaging of Implanted Window Chambers," Novel Techniques in Microscopy (NTM), NWD4 (2009).
11. C. H. Li, and L. V. Wang, "Photoacoustic tomography and sensing in biomedicine," Phys. Med. Biol. **54**(19), R59–R97 (2009).
12. J. Perez-Juste, I. Pastoriza-Santos, L. M. Liz-Marzan, and P. Mulvaney, "Gold nanorods: Synthesis, characterization and applications," Coord. Chem. Rev. **249**(17-18), 1870–1901 (2005).
13. A. Agarwal, S. W. Huang, M. O'Donnell, K. C. Day, M. Day, N. Kotov, and S. Ashkenazi, "Targeted gold nanorod contrast agent for prostate cancer detection by photoacoustic imaging," J. Appl. Phys. **102**(6), 064701 (2007).
14. S. Mallidi, T. Larson, J. Tam, P. P. Joshi, A. Karpiouk, K. Sokolov, and S. Emelianov, "Multiwavelength photoacoustic imaging and plasmon resonance coupling of gold nanoparticles for selective detection of cancer," Nano Lett. **9**(8), 2825–2831 (2009).

#129841 - $15.00 USD Received 9 Jun 2010; revised 23 Jul 2010; accepted 28 Jul 2010; published 16 Aug 2010

15. K. Kim, A. Agarwal, A. M. McDonald, R. M. Moore, D. D. Myers, R. S. Witte, S. W. Huang, S. Ashkenazi, M. J. Kaplan, T. W. Wakefield, M. O'Donnell, and N. A. Kotov, "In vivo imaging of inflammatory responses by photoacoustics using cell-targeted gold nanorods (GNR) as contrast agent," Proc. SPIE 2008 **6856**, 68560H (2008).
16. C. K. Liao, S. W. Huang, C. W. Wei, and P. C. Li, "Nanorod-based flow estimation using a high-frame-rate photoacoustic imaging system," J. Biomed. Opt. **12**(6), 064006 (2007).
17. D. R. Bauer, R. Olafsson, L. G. Montilla, and R. S. Witte, "In vivo multi-modality photoacoustic and pulse echo tracking of prostate tumor growth using a window chamber," Proc. SPIE 2010 **7564**, 75643B (2010).
18. Laser Institute of America, "American national standard for safe use of lasers Z136.1" (2000).

1. Introduction

According to the American Cancer Society approximately 192,000 U.S. citizens were diagnosed in 2009 with prostate cancer and approximately 27,000 were expected to die from the disease [1]. Better diagnosis and treatments are needed to improve this outcome. However therapeutic and imaging agents cost $800 million and $150 million to develop, respectively, making pharmaceutical development a risky business that demands a high rate of return to maintain profitability. A large portion of this development cost lies in the late stages of clinical trials [2]. It is therefore imperative to reject unpromising compounds and agents at an early stage of development. Appropriate *in vivo* experimental systems can contribute to this process.

One such system is the dorsal skin fold window chamber. It is a well established technique for *in vivo* optical and fluorescent microscopy of implanted cancers over a period of several weeks [3–5]. The model has contributed significantly to cancer research and has been extended to imaging modalities other than microscopy [6–10]. This ability for extensive cross validation with other modalities makes the window chamber ideal for the development of imaging agents. Most techniques available for imaging the window chamber provide high spatial resolution in the lateral dimension, but provide minimal depth information. As the tumor grows to several millimeters within the skin flap, depth imaging becomes especially challenging. Some techniques that can provide depth information such as magnetic resonance imaging (MRI) and optical coherence tomography (OCT) are limited in spatial resolution and penetration depth, respectively [7, 8].

Photoacoustics (PA) is a promising new imaging technique that uses ultrasonic waves generated when pulsed laser light is absorbed in tissue. PA imaging, like conventional pulse echo (PE) ultrasound is inherently a three dimensional (3D) imaging modality, offering relatively good soft tissue penetration and high axial and lateral resolution [11]. By tuning the wavelength of incident light, spectroscopic images can be acquired for characterizing tissue, tracking contrast agents or mapping blood oxygen saturation [11]. PA contrast agents are optically absorbing dyes and particles. Gold nanorods (GNRs) are particularly promising due to their strong near infrared absorption, which can be tuned by adjusting their aspect ratio [12]. They have been investigated for imaging cancer [13, 14], inflammation [15], and perfusion [16]. When more than one optical wavelength is employed, PA spectroscopy facilitates distinguishing contrast agents from other absorbing structures in the body, such as blood [14]. Photoacoustic spectroscopy, therefore, enhances specificity contributing to the photoacoustic image.

In a previous report, we described a novel platform for monitoring mouse tumors through a window chamber using multiple modalities [17]. In that study, prostate tumor invasions were monitored for 3 + weeks with high resolution PA and PE imaging combined with transillumination microscopy and fluorescent microscopy of green fluorescent protein (GFP) expressed by the tumor cells. Despite excellent depth resolution and agreement with optical methods, the PA and PE imaging platform was limited by the single element focused ultrasound transducer that required *mechanical* scanning and long acquisition times to generate two and three dimensional images. In this study, we describe a dramatic improvement to the earlier imaging platform by employing a clinical ultrasound scanner and a linear array to *rapidly* acquire ultrasound and PA images in mice implanted with a window

#129841 - $15.00 USD Received 9 Jun 2010; revised 23 Jul 2010; accepted 28 Jul 2010; published 16 Aug 2010

chamber. As we demonstrate, the fast acquisition time enables 1) real-time monitoring of contrast agents injected in mice and 2) volumetric and spectroscopic PA imaging for imaging the tumor microenvironment and detecting contrast agents with high specificity. A real-time clinical ultrasound system capable of real-time PA imaging potentially facilitates translation of the technology to humans for screening of new cancer drugs or imaging agents.

2. Methods

Human prostate cancer cells (PC3N) expressing GFP were implanted in the dorsal skin flap of a severe combined immunodeficient (SCID) mouse. The mouse was cared for in accordance with a protocol approved by the Institutional Animal Care and Use Committee (IACUC) at the University of Arizona. The prostate tumor invasion was monitored during three weeks using a dual modality PE and PA imaging system, in addition to optical and fluorescent microscopy. The experimental setup for collecting ultrasound and photoacoustic images from live mice is depicted in Fig. 1. The dorsal skin flap was stretched and held in place with a titanium window chamber with a glass coverslip on one side [4]. The skin flap was illuminated from below with a pulsed laser source (optical parametric oscillator, Surelite OPO I-20, Continuum) tunable between 680 and 1000 nm (5 nsec and 20 mJ/pulse at a repetition frequency of 20 Hz). The beam was conditioned with a two lens beam expander and directed upward with a right angle prism. The pulse energy was evenly distributed over the exposed skin within the window chamber such that incident fluence was 16 mJ/cm^2, within the ANSI safety guidelines [18].

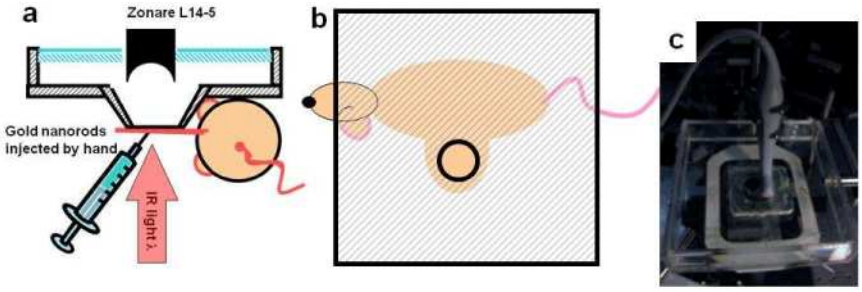

Fig. 1. Experimental setup for fast, contrast enhanced photoacoustic imaging in the mouse window chamber. a) A side view illustration with the L14-5 linear array (Zonare Medical Systems). The mouse rests on its side with the dorsal skin flap window chamber situated under a custom plastic tank. The window chamber was illuminated from below through the cover slip with near infrared (NIR) light of wavelength λ. Ultrasound and photoacoustic imaging was performed through the skin flap. Gold nanorods were manually injected into the tumor on Day 23. b) Top view of the window chamber. The mouse lies below the tank with only the window chamber skin flap exposed. c) A photograph of the L14-5 linear array positioned in the water tank above the skin flap.

To demonstrate the full capability of the enhanced imaging platform, two different ultrasound transducers were used for imaging. First, a 25 MHz *single element* ultrasound transducer (Olympus V324; center frequency = 25 MHz, focal length = 12.7 mm, f/# = 1.4) was raster scanned with a 3D motor system (Velmex) in a 6 mm by 14 mm rectangular region of interest along the x- and y-axis respectively with step sizes Δx = 100 μm and Δy = 47.6 μm. PA signals, generated with 700 nm illumination, were acquired at the same time as PE signals with a 12 bit, 62.5 MHz acquisition board (PDA12, Signatec). Following a protocol described previously [17], the single element transducer and imaging platform was used to track the tumor invasion during 3 + weeks. Three dimensional data sets were acquired on 5 separate days (7, 10, 13, 17, and 23 days after implantation). Long acquisition times (>45 minutes at a single wavelength), however, prevented volumetric and spectroscopic photoacoustic imaging in live mice. Contrast agents could not be monitored in real-time. To overcome these limitations and as a dramatic improvement to the original imaging platform,

#129841 - $15.00 USD Received 9 Jun 2010; revised 23 Jul 2010; accepted 28 Jul 2010; published 16 Aug 2010

we implemented a clinical scanner (Zonare Medical Systems) and L14-5 linear array customized for real-time photoacoustic imaging. Three dimensional data were obtained with the 14 MHz transducer by translating it orthogonal to its image plane along the y-axis. Since the 14 MHz probe allowed for simultaneous acquisition of in phase and quadrature (IQ) data on 64 elements (half aperture) with each laser pulse, the acquisition of a 3D PA data (30 mm axial, 12.5 mm lateral, 20 mm elevational) took only 20 seconds for each wavelength. The IQ data was interpolated, upmodulated to 10 MHz, and bandpass filtered in fast time with −6dB cutoff frequencies of 7.5 and 12.5 MHz. A sum delay beamforming algorithm was used to produce volumetric 3D scans, which were further median filtered in the lateral direction with a 5x5 pixel window. The resulting data was logarithmically compressed for display.

To demonstrate the full capabilities of the enhanced imaging platform and clinical scanning system, a 10 nM solution of gold nanorods (GNRs, 45 nm x15 nm, peak absorption near 780 nm) was injected into the mature mouse tumor on Day 23. The absorption spectrum of the nanorods was independently measured with a commercial spectrometer (USB4000, Ocean Optics). The injection site was monitored in real-time (at the laser repetition frequency of 20 Hz) for 30 seconds at 700 nm illumination. A 3D PA and PE data set was acquired before and after the injection at 10 different wavelengths (λ = 680-900 nm, $\Delta\lambda$ = 25 nm). The vasculature and structure of the skin was captured with an optical transillumination and fluorescent microscope, which also assessed the distribution of tumor cells expressing GFP (Eclipse E600, Nikon). The clinical ultrasound system not only enabled real-time tracking of photoacoustic contrast agents, but it also acquired images fast enough to obtain volumetric, spectroscopic photoacoustic images in living mice with high enhanced detection specificity of GNRs.

3. Results

Figure 2 illustrates the growth of the tumor over three weeks captured by the slow single element, mechanical scanning system (PA and PE), as well as the corresponding optical and fluorescent images. Results were consistent with prostate tumor growth observed in previous mice implanted with a similar window chamber [17]. Since the tumor cells expressed GFP, fluorescent images provided a gold standard for the lateral extent of the cancer. The transillumination images depicted primarily the blood vasculature. They also reveal that the skin flap had started to detach as the tumor grew. Cross sectional PE (gray scale) and PA images (hot scale) are part of a 3D data set and correspond to the center of the window chamber. Using the PE images, the growth of the tumor can be quantified. In this example, the tumor grew from 0.5 mm thickness on day 7 post implantation to 5 mm on day 23. That is, the tumor was 10 times thicker on the last day compared to the first. The PA images, obtained with 700 nm illumination and superimposed on the PE images, appeared as discrete hot spots. and represent cross sections of the blood vessels. Therefore, PE and PA images provide complementary contrast.

However, the long acquisition time (40 + minutes) for each wavelength using the single element transducer precluded using it for 3D spectroscopic photoacoustic imaging or real-time dynamic 2D imaging with contrast agents. The clinical ultrasound scanner and 14 MHz array, on the other hand, acquired 2D frames at 20 Hz, limited only by the pulse repetition rate of the laser. This real-time system permitted the acquisition of 3D images of the entire window chamber every 20 seconds per wavelength, or approximately *120 times faster* than the single element transducer. To demonstrate enhanced imaging of the mouse window chamber with contrast agents, real time PA imaging was performed before, during and after the injection of GNRs into the tumor as illustrated in Fig. 3. Figure 3b also displays a cross sectional pulse echo image (B-mode) acquired using the same system before the real-time PA imaging. Figure 3c represents the space vs. time PA image (M-Mode) in a plane through the shaft of

#129841 - $15.00 USD Received 9 Jun 2010; revised 23 Jul 2010; accepted 28 Jul 2010; published 16 Aug 2010

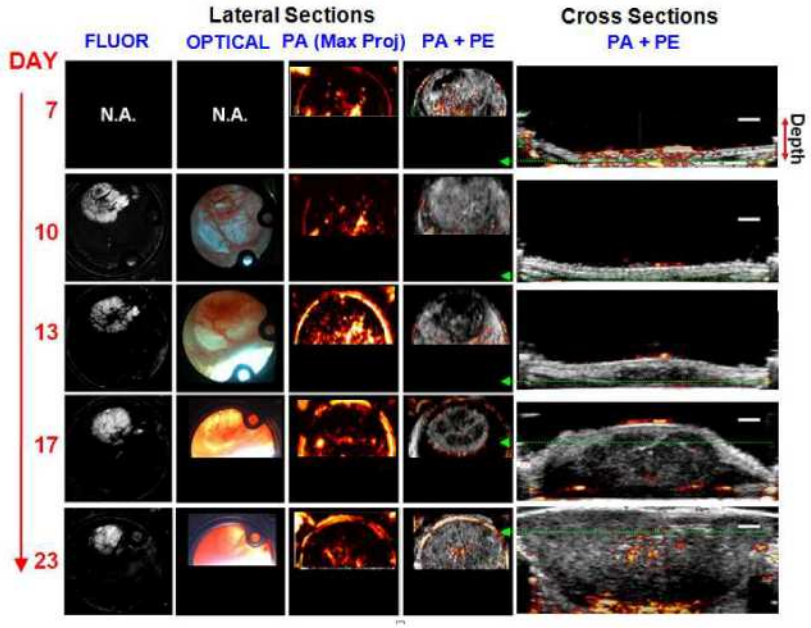

Fig. 2. Example: tracking tumor progression during 3 weeks using multiple modalities. (left column) Fluorescent (Fluor) and (middle left column) optical transillumination (Optical) microscope images acquired on the same day as the pulse echo (PE) and photoacoustic (PA) images. (middle column) lateral maximum intensity projection PA images. (middle right column) lateral PA slices superimposed on PE slices. (right column) PA cross sections superimposed on PE. The horizontal green arrows correspond to the depth of the lateral slices in the middle right column. PE images are grayscale while PA are superimposed in hot scale. These images were acquired with a high resolution single element 25 MHz transducer. The white scale bar is 1 mm.

the injection needle, corresponding to the vertical green dashed line of the initial PA cross sectional image (depicted in Fig. 3a). In this image, a quick bolus can be discerned at the time of injection, followed by a gradual increase in image intensity with time. This increase is illustrated more quantitatively in Fig. 3d, where the image intensity along the green dashed line (in Fig. 3c) increased by 10 dB after 30 seconds. Figure 4 depicts three orthogonal planes from a volumetric PA image acquired at 700 nm immediately after the injection of GNRs and exhibits the distribution of nanorods near the tumor, as well as endogenous contrast from blood vessels. The XY lateral view clearly depicts the circular outline of the window chamber.

Spectroscopic PA XY images acquired before and after the injection of the GNRs are shown in Fig. 5. In these lateral views from a spectroscopic and volumetric data set, the circular outline of the window chamber can also be discerned. In the central region, there is an increase in image intensity after the injection compared to before the injection. The spectral plot in Fig. 6 describes the change in PA signal intensity as a function of laser wavelength. The difference in logarithmic image intensity (i.e., gain) between the “before” and “after” spectroscopic PA images in the region of interest (denoted by a green rectangle) is clearly different than the spectrum measured in a control region located in the upper right corner. The injection of GNRs produced an 18 dB signal increase at the 825-850 nm wavelength (within the region of interest) compared to an average gain of 0.8 dB in the control region far away from the injection. This strongly suggests that the observed increase in image intensity was primarily due to the presence of GNRs in region near the tumor.

#129841 - $15.00 USD Received 9 Jun 2010; revised 23 Jul 2010; accepted 28 Jul 2010; published 16 Aug 2010

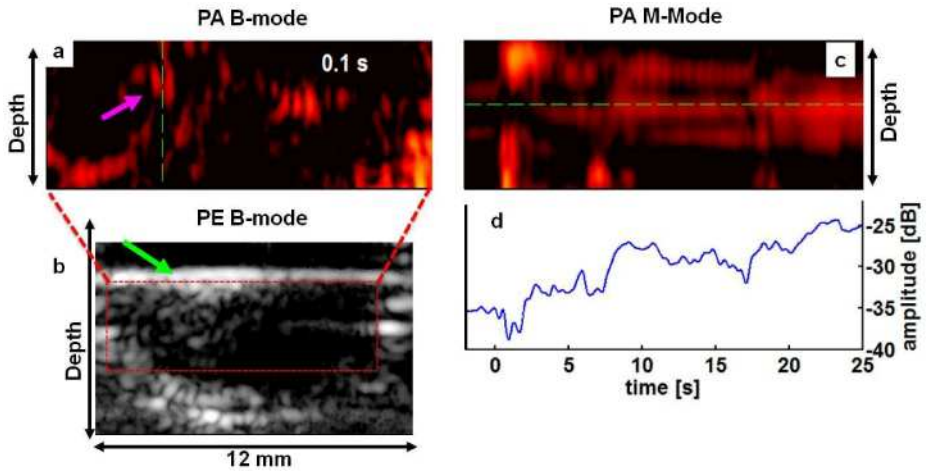

Fig. 3. Photoacoustic data acquired during injection of gold nanorods. a) An image captured 100 msec after the start of the GNR injection. The pink arrow illustrates the shaft of the needle used for the injection. This image corresponds to the red dashed rectangle in the grayscale pulse echo image b) The green arrow (top) points to the Tegaderm™ acoustic window. The bottom of the skin (bottom) is sagging because the glass coverslip was removed to permit access for the injection needle. The 30 dB dynamic range and the hot colorscale are the same as in Fig. 4. Image c) is a depth vs. time (M-mode) PA image illustrating the evolution of the PA signal at the location of the vertical green dotted line in image a). The plot in d) is the signal intensity as a function of time along the horizontal green line in image c).

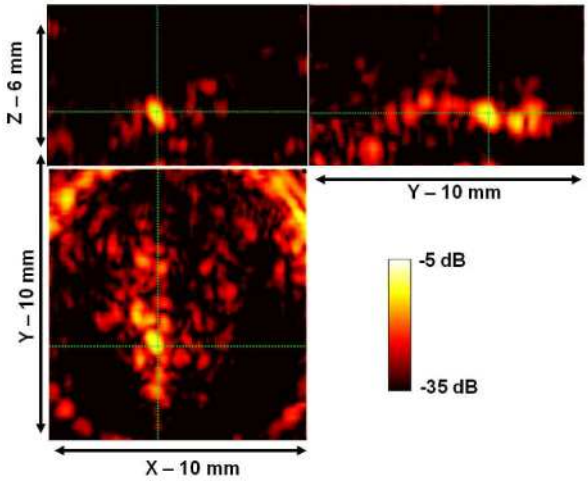

Fig. 4. Example: Orthogonal planes from a three dimensional photoacoustic data set of nanorods injected into a tumor acquired with the real-time clinical scanner and 14 MHz clinical array using 700 nm illumination. The three orthogonal images were selected in the region near the tumor and site of GNR injection.

#129841 - $15.00 USD Received 9 Jun 2010; revised 23 Jul 2010; accepted 28 Jul 2010; published 16 Aug 2010

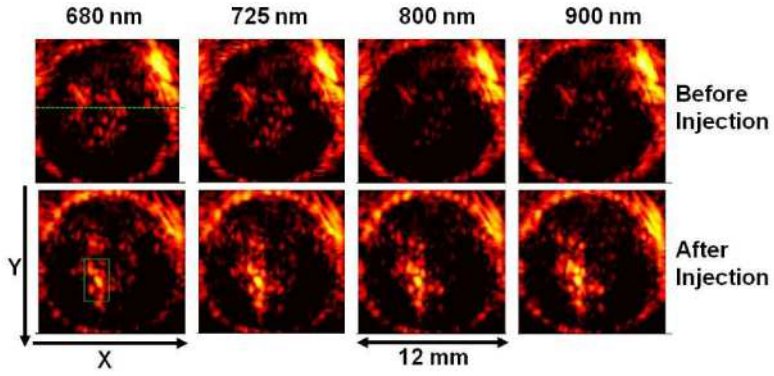

Fig. 5. Lateral slices form a multispectral 3D photoacoustic data set acquired with the clinical linear array. Photoacoustic slices were acquired before (top row) and after (bottom row) the injection of GNRs. Each column represents images taken at a particular excitation wavelength (four representative wavelengths displayed). The horizontal green dashed line corresponds to the image cross section shown in Fig. 3.

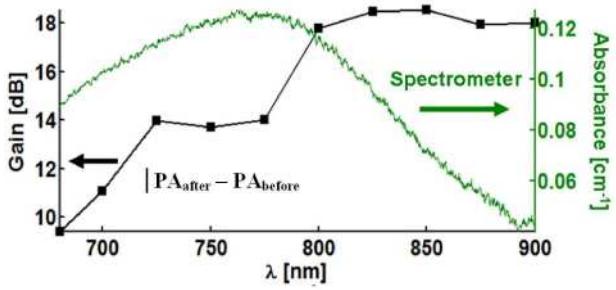

Fig. 6. Optical absorption spectrum of GNRs before the injection and changes in the photoacoustic spectrum in the region of interest following the injection of GNRs. The plot with the black squares on the right is the gain in average image intensity within the green rectangle in Fig. 5 primarily due to the nanorods. The green line represents the absorption spectrum of the nanorods measured with a commercial spectrometer.

4. Discussion

We have demonstrated real time and contrast enhanced photoacoustic imaging and spectroscopy of a mature prostate tumor in a mouse window chamber model using a clinical ultrasound system and 14 MHz linear array. Although our original single element PA and PE imaging system was able to track tumor invasions in SCID mice at high spatial resolution (as depicted in Fig. 2), the enhanced system is approximately 120 times faster and provided new opportunities for 3D spectroscopic PA imaging in live mice. The experimental system not only facilitates testing new PA contrast agents and drug delivery using a preclinical model, but the enhanced hardware could help accelerate translation of this emerging technology to cancer patients. The clinical scanner and linear array, for example, could potentially provide photoacoustic imaging and spectroscopy through the skin of mice or humans for cancer research and imaging. The system is also capable of real-time pulse echo and photoacoustic imaging, thereby providing complementary contrast related to tumor identification and volumetric growth (PE), as well as the tumor neovasculature (PA without contrast agents). Despite a slightly lower spatial resolution than the single element platform, this study opened new possibilities for real-time, contrast enhanced photoacoustic imaging. We were able to dynamically track the injection of PA contrast agents into the tumor, as illustrated in Fig. 3 and observed a 10 dB increase in PA intensity within 30 seconds near the injection. Whereas the PE image provided anatomical reference at the injection site, the co-registered PA images also visualized the needle and dynamically tracked the distribution of GNRs. This provides

#129841 - $15.00 USD Received 9 Jun 2010; revised 23 Jul 2010; accepted 28 Jul 2010; published 16 Aug 2010

support for potentially using such a system to guide injections in real-time. Previous work describing PA perfusion imaging tracked GNRs in a plastic tube phantom embedded in externalized tissue, but not in an in vivo mouse model for prostate cancer. Other studies using ultrasound arrays to track the distribution of GNRs *in vivo* were not typically part of a clinical scanning system [16]. Although clinical scanners that have been used previously to image GNRs tagged to prostate tumor cells in gelatin implanted in a mouse [13], the slow acquisition speed in these studies enabled only static 2D images acquired at a single wavelength. The clinical scanner we used permitted real time and 3D imaging as illustrated by Figs. 3, 4, and 5. As depicted by the multispectral data in Fig. 6, the injection of GNRs increased the PA signal intensity between 10 and 18 dB in the tumor, depending on the wavelength. By comparison the intensity in the control region changed less than 1 dB, indicating that the increase in intensity was specific to the site of the injection. The peak of the spectrum measured with PA was slightly redshifted by 50 nm compared to the spectrum measured with the commercial spectrometer. The enhanced signal >800 nm may be partially due to the fact that light travelled through 5 + mm of tissue with wavelength dependent absorption before reaching the nanorods. It could also be related to aggregation or surface effects of the nanorods in the tissue compared to the buffered saline environment for the measurement in the spectrometer [12, 14]. Nonetheless, the absorption profile of GNRs is distinct and differs from background photoacoustic signals (e.g., blood) [14].

The window chamber model integrated with a clinical ultrasound scanner is useful for developing photoacoustic imaging technology and screening new cancer drugs or contrast agents. The window chamber permits independent verification of the targeting and binding of agents, as well as detailed characterization of tumor proliferation or regression. In addition to the enhanced acquisition capabilities that a linear array provides, a commercial ultrasound scanner makes it is possible to assess the *in vivo* sensitivity and spectrum of the contrast agents using a similar system already available for routine ultrasound exams. This can potentially facilitate the translation of imaging technology and drug discovery from benchtop to bedside.

We plan to continue to improve our system in future studies. Rather than injecting directly into the tumor, future studies will involve contrast agent injections directly into the mouse venous system and using GNRs with molecular markers targeted for cancer imaging.

5. Conclusions

In this study, we demonstrated a major enhancement to a photoacoustic and ultrasound imaging platform designed to track prostate tumors in SCID mice implanted with a window chamber. A clinical ultrasound scanner and linear array enabled real time PA imaging during the injection of GNRs into a mature prostate tumor. The tumor region was further visualized with volumetric PA imaging and spectroscopy before and after the injection, providing additional information related to the origin of the PA signal and spectral content of the GNRs near the tumor. The enhancement to the experimental model and imaging platform potentially accelerates the development of diagnostic and therapeutic agents for cancer.

Acknowledgements

This was supported in part by the Arizona Cancer Center IRG-7400128, NSF 0853618, Advanced Research Institute for Biomedical Imaging (ARIBI), and Technology Research Infrastructure Fund (TRIF). We would like to thank Gillian D. Paine-Murrieta, Bethany Skovan and the Experimental Mouse Shared Service (EMSS) for attaching the mouse window chamber and the implantation of the tumor. We thank Christine Howison and Michael Bernas for their help with the animal preparation and Prof. Art Gmitro's laboratory for help with their fluorescent microscope. Finally, we also would like to acknowledge Zonare Medical Systems for technical support related to the clinical scanner.

#129841 - $15.00 USD Received 9 Jun 2010; revised 23 Jul 2010; accepted 28 Jul 2010; published 16 Aug 2010